JOURNAL OF GEOPHYSICAL RESEARCH, VOL. 95, NO. D2, PAGES 1837–1851, FEBRUARY 20, 1990

# The Sensitivity of Ozone to Nitrogen Oxides and Hydrocarbons in Regional Ozone Episodes

SANFORD SILLMAN,[1] JENNIFER A. LOGAN, AND STEVEN C. WOFSY

*Department of Earth and Planetary Sciences and Division of Applied Sciences*
*Harvard University, Cambridge, Massachusetts*

We examine the sensitivity of ozone concentrations in rural areas of the United States to emissions of $NO_x$ and hydrocarbons using a regional photochemical model. Ozone production in rural areas appears to be limited by the availability of $NO_x$. Rural ozone is strongly dependent on emission rates for $NO_x$ but is almost independent of hydrocarbons. This relationship is quite different from that in urban air, where ozone levels depend on both $NO_x$ and hydrocarbons. The predicted relationship between ozone and nitrogen oxides appears to be consistent with observations in rural air. For the low $NO_x$ regime (<2 ppb) in rural areas, increases in $NO_x$ lead to increases in OH and to corresponding increases in the oxidation rate of hydrocarbons and in levels of ozone. Ozone concentrations in urban plumes appear to be related to regional scale production in addition to production within the plume.

## 1. INTRODUCTION

Ozone concentrations in rural areas of the industrialized continents are considerably higher than values found in locations remote from anthropogenic activity [e.g., *Logan*, 1985, 1989]. Ozone concentrations in rural locations in Europe appear to be increasing [*Warmbt*, 1979; *Attmannspacher et al.*, 1984; *Logan*, 1985; *Feister and Warmbt*, 1987]. According to *Volz and Kley* [1988] levels today are more than double values found 100 years ago. Particularly high values of ozone (>90 ppb) tend to occur during pollution episodes of large spatial scale (>500,000 $km^2$), between the months of April and September. These episodes persist for 3-4 days on average and recur several times each year [*Logan*, 1989]. They are generally associated with slow-moving high-pressure systems, when meteorological conditions are conducive to photochemical formation of ozone, with warm temperatures, clear skies, and low wind speeds [e.g., *Cox et al.*, 1975; *Research Triangle Institute*, 1975; *Decker et al.*, 1976; *Vukovich et al.*, 1977; *Wolff et al.*, 1977; *Guicherit and van Dop*, 1977; *Wolff and Lioy*, 1980].

Elevated levels of ozone are harmful to human health and to vegetation. Recent studies suggest that exposure to concentrations of 120 ppb, the current national ambient air quality standard in the United States, may be harmful for exercising individuals [*Folinsbee et al.*, 1988]. Field studies have shown that yields of agricultural crops decrease as ozone increases, with reductions of 6-8% per 10 ppb of ozone [*Heck et al.*, 1982]. Exposure to the high ozone values found during episodes may be particularly damaging [e.g., *Environmental Protection Agency (EPA)*, 1986*a*; *Lefohn and Runeckles*, 1987]. Several species of trees are susceptible to damage by ozone, and there is concern that ozone may be contributing to the decline of forests in Europe and in the eastern United States [*Skarby and Sellden*, 1984; *Woodman and Cowling*, 1987].

Considerable attention has been devoted to the problem of elevated levels of ozone in urban areas [e.g., *EPA*, 1986*a*], but the problem of rural ozone has received much less attention. Pioneering studies by *Hov et al.* [1978] and *Isaksen et al.* [1978] showed that ozone may build up to values of 100-180 ppb in a few days in rural air subject to anthropogenic emissions of $NO_x$ and hydrocarbons. The ozone produced in this way can persist for several days, permitting long-range transport. These authors showed also that oxidation of $CH_4$ alone is insufficient to raise the level of ozone above 60 ppb and that nonmethane hydrocarbons (anthropogenic or natural) are required to produce higher values. More recently, *Liu et al.* [1987] showed that oxidation of hydrocarbons was required to explain the relationship between ozone and $NO_x$ at Niwot Ridge, Colorado, a remote site impacted by urban plumes. They demonstrated that the relationship between ozone and $NO_x$ is non linear and that ozone production per unit $NO_x$ is greater for lower $NO_x$ [see also *Lin et al.*, 1988]. *Trainer et al.* [1987a] investigated the role of natural hydrocarbons on ozone at a rural site in the eastern United States and concluded that oxidation of biogenic isoprene, in the presence of anthropogenically emitted $NO_x$, can lead to ozone concentrations exceeding 100 ppb. *Selby* [1987] examined ozone formation in Europe using meteorological data for anticyclonic episodes [*van Dop et al.*, 1987]. He calculated the evolution of ozone along 3-day wind trajectories and examined the sensitivity of ozone to changes in emissions of $NO_x$ and hydrocarbons; he found that ozone becomes less sensitive to hydrocarbons as a polluted air mass moves into an area of low emissions and that ozone is controlled eventually by the availability of $NO_x$ in regions removed from sources.

In this study we examine the sensitivity of ozone in rural areas of the eastern United States to emissions of $NO_x$ and hydrocarbons. First, we use a simple two-layer model to illustrate the sensitivity of rural ozone to emissions of $NO_x$ and hydrocarbons, and to elucidate the chemical mechanisms responsible for the non linear dependence of ozone on precursor emission rates. We then use a regional scale model for the northeastern United States [*Sillman et al.*, 1990] to explore the factors that influence ozone in rural areas during stagnation periods, again focusing on precursor emission rates. Finally, we use a fine-resolution Eulerian grid model to predict the relationship between ozone, $NO_x$ and $NO_y$, and we compare model results with field data. We begin with a discussion of the photochemistry of ozone.

[1] Now at Department of Atmospheric, Oceanic, and Space Sciences, University of Michigan, Ann Arbor.



Paper number 89JD01645.
0148-0227/90/89JD-01645$05.00

## 2. CHEMISTRY OF OZONE

Ozone is a product of the photochemical oxidation of CO, $CH_4$ and higher hydrocarbons (RH) in the presence of $NO_x$. The mechanism is simplest for CO:

$$\text{(R1)} \quad OH + CO \xrightarrow{[O_2]} HO_2 + CO_2$$

$$\text{(R2)} \quad HO_2 + NO \rightarrow OH + NO_2$$

$$\text{(R3)} \quad NO_2 + h\nu \rightarrow NO + O$$

$$\text{(R4)} \quad O + O_2 + M \rightarrow O_3 + M$$

$$\text{Net:} \quad CO + 2O_2 + h\nu \rightarrow CO_2 + O_3$$

The oxidation pathways for hydrocarbons are more complex but follow a sequence analogous to (R1)-(R4), as discussed in more detail by *Atkinson* [1986]:

$$\text{(R5)} \quad OH + RH \xrightarrow{[O_2]} RO_2 + H_2O$$

$$\text{(R6)} \quad RO_2 + NO \xrightarrow{[O_2]} NO_2 + HO_2 + CARB$$

$$\text{(R2)} \quad HO_2 + NO \rightarrow OH + NO_2$$

$$\text{(R3)} \quad 2(NO_2 + h\nu \rightarrow NO + O)$$

$$\text{(R4)} \quad 2(O + O_2 + M \rightarrow O_2 + M)$$

$$\text{Net:} \quad RH + 4O_2 + h\nu \rightarrow 2O_3 + CARB$$

CARB represents a carbonyl or aldehyde; subsequent reactions may lead to further generation of ozone and may also provide a source of odd hydrogen, as discussed below. Reactions (R2) and (R6) break the O-O bond; these are the major reaction paths for $HO_2$ and $RO_2$, respectively, when $NO_x$ exceeds ~0.3 ppb. It is important to note that $NO_x$ plays the role of a catalyst in the reaction sequences shown above, while the carbon compounds are consumed, eventually being oxidized to $CO_2$. The number of ozone molecules produced by oxidation of a given hydrocarbon depends on its structure and on atmospheric composition; for the species found in ambient air, containing 2-6 carbon atoms, each molecule may generate 4-14 ozone molecules [*Singh et al.*, 1981]. Oxidation of unsaturated hydrocarbons may be initiated by reaction of ozone with RH, but this usually represents a minor pathway for the mix of hydrocarbons found in ambient air.

The major photochemical paths for removal of ozone are photolysis followed by reaction of $O(^1D)$ with water vapor, reaction of $HO_2$ with ozone, and formation of nitric acid, which is a chain-terminating step for $NO_x$ radicals,

$$\text{(R7)} \quad O_3 + h\nu \rightarrow O(^1D) + O_2$$

$$\text{(R8)} \quad O(^1D) + H_2O \rightarrow OH + OH$$

$$\text{(R9)} \quad HO_2 + O_3 \rightarrow OH + 2O_2$$

$$\text{(R10)} \quad OH + NO_2 + M \rightarrow HNO_3 + M$$

Ozone is removed also by dry deposition, and this represents the major removal process from the boundary layer over land [*Wesely*, 1983].

Chemical mechanisms for the oxidation of hydrocarbons are complex. Here we derive simplified expressions for the production rate of ozone from $NO_x$ and hydrocarbons for limiting cases of high and low $NO_x$. We will see below (section 4) that these expressions provide a good description of the sensitivity of ozone production to $NO_x$ and hydrocarbons in rural air.

The rate-limiting step for the rate of ozone production is the reaction of OH with CO or with hydrocarbons, reactions (R1) and (R5); the key process that results in the formation of ozone is the reaction of $HO_2$ with NO, reaction (R2). Odd-hydrogen radicals therefore play a key role in ozone production, and it is useful to examine the factors that control OH and $HO_2$. Following *Kleinman* [1986], we use a definition of odd-hydrogen radicals that includes $RO_2$ and $RCO_3$ species (e.g., $CH_3O_2$, $CH_3CO_3$) in addition to OH and $HO_2$. With this definition, odd hydrogen is conserved in reactions (R5) and (R6). Hydrogen peroxide, other organic peroxides, and peroxyacetylnitrate (PAN) and its homologues (peroxyacyl nitrates with longer carbon chains) are reservoirs for the odd-hydrogen radicals. The major sources for odd hydrogen are reaction (R8) and photolysis of formaldehyde, higher aldehydes and carbonyls:

$$\text{(R11)} \quad H_2CO + h\nu \rightarrow H + HCO$$

$$\text{(R12)} \quad HCO + O_2 \rightarrow HO_2 + CO$$

$$\text{(R13)} \quad RCHO + h\nu \rightarrow H + RCO$$

The H atom formed in (R11) and (R13) immediately combines with $O_2$ to form $HO_2$. Reaction with OH represents the major sink for acetaldehyde ($CH_3CHO$) and higher aldehydes (RCHO); photolysis provides an additional sink for formaldehyde, methylgloxyl and other dicarbonyls. Consequently, the steady state concentration of RCHO is proportional to RH but independent of OH; the concentration of $H_2CO$ and dicarbonyl species is also proportional to RH but depends weakly on OH.

Major sinks for odd-hydrogen radicals include formation of hydrogen peroxide and higher peroxides, formation of nitric acid, and formation of PAN and its homologues:

$$\text{(R14)} \quad HO_2 + HO_2 \rightarrow H_2O_2 + O_2$$

$$\text{(R15)} \quad RO_2 + HO_2 \rightarrow ROOH + O_2$$

$$\text{(R10)} \quad NO_2 + OH \xrightarrow{M} HNO_3$$

$$\text{(R16)} \quad RCO_3 + NO_2 \xrightarrow{M} PAN$$

Analysis of the reactions above allows derivation of a useful approximation for the odd-hydrogen balance. If we recognize that the rate of PAN formation is proportional to the rate of reaction of hydrocarbons with OH, (R5), (see below), the odd-hydrogen balance may be expressed as

$$A[O_3] + B_1[RH] + B_2[OH][RH] = 2k_{14}[HO_2]^2 + 2k_{15}[HO_2][RO_2] + k_{10}[OH][NO_2] \quad (1)$$

where the $A$ term accounts for the source for odd H from photolysis of ozone, the $B_1$ term accounts approximately for the source from photolysis of aldehydes, and the $B_2$ term is a composite that accounts for the source from formaldehyde and dicarbonyls, $C_1$[OH][RH], and the odd-H sink from PAN formation, $C_2$[OH][RH] (i.e., $B_2 = C_1 - C_2$). Values for $B_1$, $C_1$, and $C_2$ depend on the hydrocarbon mix, temperature, radiation, and details of the chemical mechanism. Typical values for $A$, $B_1$, $C_1$, and $C_2$ at 1200 LT determined empirically from simulations with the mechanism of *Lurmann et al.* [1986] for ambient summer conditions are $A = 4\text{x}10^{-6}$ s$^{-1}$; $B_1 = 3\text{x}10^{-6}$ s$^{-1}$; $C_1 = 2\text{x}10^{-13}$ cm$^3$ s$^{-1}$; $C_2 = 5.5\text{x}10^{-13}$ cm$^3$s$^{-1}$.

Approximate solutions to equation (1) may be obtained for the limiting cases of high or low concentrations of $NO_x$, using the ratio of OH to $HO_2$ implied by reactions (R1), (R2), (R5) and (R6),

$$\frac{[OH]}{[HO_2]} = \frac{k_2[NO]}{k_1[CO] + k_5[RH]} \quad (2)$$

Here $k_5$ is the concentration-weighted mean rate for reaction of OH with the ambient mix of hydrocarbons. For high concentrations of $NO_x$ (>4 ppb) with RH < 100 ppb, the dominant sink for odd H is formation of nitric acid, and the peroxide sinks may be ignored. The resulting solution for OH is

$$[OH] = \frac{A[O_3] + B_1[RH]}{k_{10}[NO_2] - B_2[RH]} \quad (3)$$

Production of ozone is proportional to the rate of reactions (R1) and (R5):

$$P[O_3] \sim [OH](k_1[CO] + k_5[RH]) \approx k_2[HO_2][NO] \quad (4)$$

Thus

$$P[O_3] \sim \frac{(A[O_3] + B_1[RH])(k_1[CO] + k_5[RH])}{k_{10}[NO_2] - B_2[RH]} \quad (5)$$

Equation (5) shows that for the high-$NO_x$ case, production of ozone and concentrations of OH and $HO_2$ increase with increasing concentrations of hydrocarbons and decrease with increasing $NO_x$. The sensitivity to $NO_x$ and hydrocarbons reflects the role of the former as a sink and the latter as a source of odd-H radicals. In addition to providing a sink for odd H, formation of $HNO_3$ also provides an important photochemical sink for odd oxygen at high $NO_x$.

Different relationships obtain at low $NO_x$ concentrations (~0.3-2 ppb). Formation of peroxides represents the dominant sink for odd hydrogen. An approximate solution to equation (1) for this case is

$$A[O_3] + B_1[RH] = 2k_{14}[HO_2]^2 \quad (6)$$

$$[OH] = \frac{k_2}{(2k_{14})^{1/2}} \frac{(A[O_3] + B_1[RH])^{1/2}[NO]}{(k_1[CO] + k_5[RH])} \quad (7)$$

$$P[O_3] \sim \frac{k_2}{(2k_{14})^{1/2}} (A[O_3] + B_1[RH])^{1/2}[NO] \quad (8)$$

We see that at low $NO_x$ levels the rate of production of ozone increases proportionally with $NO_x$ and shows only a slight positive dependence on the hydrocarbon concentration; a more exact solution to the odd-H balance shows the same dependence on $NO_x$ and an even weaker dependence on hydrocarbons. Equation (8) can be understood by examining the major reaction pathways for $HO_x$. An increase in $NO_x$ causes an increase in OH (see reaction (R2)) but has no effect on $HO_2$, since the concentration of $HO_2$ is fixed by the odd-H balance given in (6); an increase in RH causes a decrease in OH but has little effect on $HO_2$, and hence production of ozone (which depends on the product of OH and RH) is rather insensitive to the concentration of RH. The major photochemical sink for ozone at low $NO_x$, photolysis of ozone (R7) followed by (R8), is independent of $NO_x$ and RH.

The chemistry of PAN may have a major effect on $NO_x$ levels and on ozone production [e.g., *Hendry and Kenley*, 1979]. PAN is produced by reaction of acetaldehyde, $CH_3CHO$, with OH and $O_2$ to form $CH_3CO_3$, which combines with $NO_2$ to form PAN:

$$\text{(R17)} \quad CH_3CHO + OH \xrightarrow{[O_2]} CH_3CO_3 + H_2O$$

$$\text{(R18)} \quad CH_3CO_3 + NO_2 \xrightarrow{M} PAN$$

The dominant removal mechanisms involve thermal decomposition followed by reaction of $CH_3CO_3$ with NO:

$$\text{(R19)} \quad PAN \xrightarrow{M} CH_3CO_3 + NO_2$$

$$\text{(R20)} \quad CH_3CO_3 + NO \xrightarrow{[O_2]} CH_3O_2 + CO_2 + NO_2$$

Reaction (R18) is extremely dependent on temperature. For typical summer temperatures (>300 K), the lifetime of PAN is short [*Cox and Roffey*, 1977] and PAN may be assumed to be in steady state: the rates of reactions (R17) and (R18) must be equal in this case, as are the rates of (R16) and (R19). Hence,

$$[PAN] = \frac{k_{17}\,k_{18}}{k_{19}\,k_{20}}[OH][CH_3CHO]\frac{[NO_2]}{[NO]} \quad (9)$$

Adopting the steady state relationship for ozone, NO, and $NO_2$,

$$[PAN] = \frac{k_{17}\,k_{18}\,k_{21}}{k_{19}\,k_{20}\,j_3}[OH][CH_3CHO][O_3] \quad (10)$$

where (R21) is

$$\text{(R21)} \quad NO + O_3 \rightarrow NO_2 + O_2$$

Equation (10) shows that the concentration of PAN increases as ozone increases. PAN may help regulate production of ozone, providing an important reservoir for $NO_x$ and for odd-hydrogen radicals, particularly at low temperatures. The influence of PAN formation on ozone at low temperatures is discussed further in section 5.

## 3. Model Description

The three atmospheric models used in this study employ the complete chemical mechanism devised by *Lurmann et al.* [1986] with minor modifications introduced by *Jacob and Wofsy* [1988] to extend its applicability to concentrations of $NO_x$ below 1 ppb. This mechanism provides a detailed treatment of chemistry for a wide variety of anthropogenic hydrocarbons and for the biogenic hydrocarbon, isoprene. The mechanism has been tested extensively by comparison with smog chamber experiments and with urban observations [*Lurmann et al.*, 1986; *Sillman*, 1987] and has been used to simulate the photochemistry of the boundary layer over the Amazon forest [*Jacob and Wofsy*, 1988]. Half-hour time steps were used in integrating the differential equations for the mechanism, using an implicit (backward Euler) algorithm.

Photolysis rates were calculated for clear sky conditions for 40°N latitude in July using the Harvard photochemical model [*Logan et al.*, 1981]. Absorption cross sections, quantum yields and solar flux data were taken from *DeMore et al.* [1985], and we adopted a total ozone column of 325 Dobson Units and surface albedo of 0.15. Absorption by aerosols was treated as discussed by *Logan et al.* [1981; Appendix 3]; the aerosol optical depth was 0.68, based on turbidity data from the eastern United States [*Flowers et al.*, 1969] and the single scattering albedo was 0.75. Photolysis rates were calculated for the midpoint of each model layer. We assumed an average surface temperature of 298 K and allowed for temperature variations with time of day and altitude as described by *Sillman et al.* [1990].

Emission rates for anthropogenic species were taken from the National Acid Precipitation Assessment Program (NAPAP) inventory, version 5.2, for a typical summer weekday [*EPA*, 1986*b*].

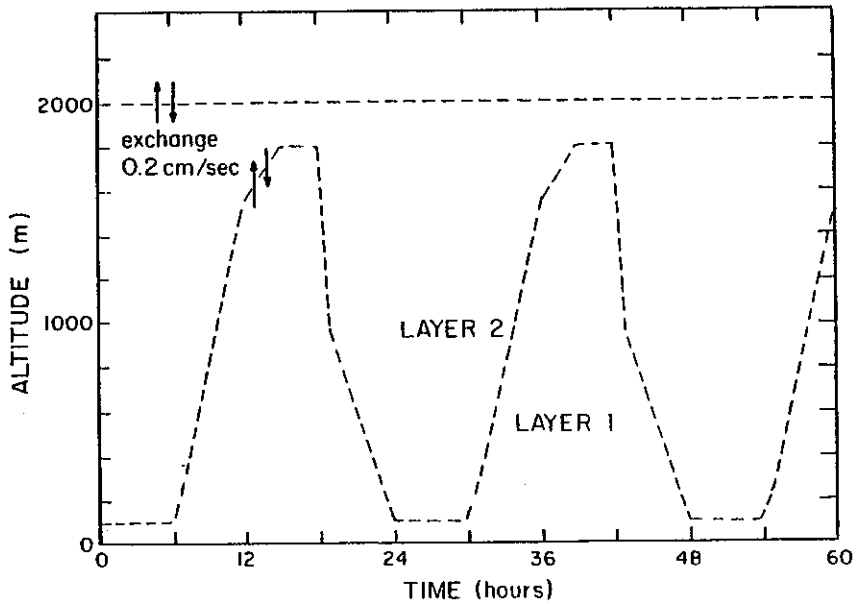


Fig. 1. Diagram of the two-layer vertical structure. The diurnal variation of the boundary layer is from the work by *van Ulden and Holtslag* [1985].

Emissions of $NO_x$ and anthropogenic hydrocarbons were assumed to vary with time of day according to average diurnal patterns [*EPA*, 1986*b*]. Emission rates for isoprene were estimated from the analysis of *Lamb et al.* [1987] which provides rates for different types of vegetation and from data for land use [*Matthews*, 1983]. The diurnal variation of the emission rate was taken from the formulation given by *Jacob and Wofsy* [1988], which allows for the dependence on solar radiation and temperature. Biogenic emissions of $NO_x$ were not included.

### 3.1. *Two-Layer Model*

A two-layer box model, shown in Figure 1, was used to elucidate the sensitivity of ozone to concentrations of its precursors, $NO_x$ and hydrocarbons. The height of the lower or mixed layer was assumed to vary diurnally, from 100 m in the early morning to 1800 m in the afternoon, as described by *van Ulden and Holtslag* [1985]. Species produced during the day are trapped in the upper layer, isolated from deposition, at night. They are entrained into the lower layer the following day. We used an exchange coefficient between the upper model layer and the free troposphere of 0.2 cm $s^{-1}$ as appropriate for stagnant conditions (see section 4 below). Emission and deposition rates provide flux boundary conditions at the bottom of the mixed layer. Deposition velocities are given in Table 1. Uniform species concentrations were assumed over the model domain at the beginning of each simulation, as given in Table 1; these values were adopted also for the upper boundary. The partitioning of hydrocarbon emissions into the species in the *Lurmann et al.* [1986] mechanism is given in Table 2.

### 3.2. *The Plumes Model*

The plumes model, a regional model, was used to examine the sensitivity of ozone in the rural eastern United States to emissions of $NO_x$ and hydrocarbons. The model uses a coarse grid resolution of 400 x 480 $km^2$ (4° latitude x 5° longitude) with a subgrid structure designed to incorporate the effects of urban-scale photochemical processes within a regional grid [*Sillman et al.*, 1990]. Each 400 x 480 $km^2$ region is divided into subregions representing (1) urban plumes within the region, (2) power plant plumes, and (3) rural locations. The urban subregion is represented by simulation of "generic" urban plumes with emissions equal to the average for all urban sources within the region; the initial width of the urban subregion is based on the largest metropolitan area in the region. Similarly, the power plant subregion is represented by generic plumes with emissions equal to the average for power plant sources. Emission rates in the rural sub region are derived by omitting sources designated as contributing to the urban or power plant subregions. Each plume is simulated for 12 hours downwind from its source. At the end of the 12-hour period the plume contents are exported to the rural subregion. New plumes are started at 4-hour intervals with initial conditions derived from the rural subregion. We have shown elsewhere that average concentrations of species in the 400 x 480 $km^2$ box calulated with the plumes model agree with results of a higher resolution (40 x 40 $km^2$) model; the two models give similar results also for the 98th percentile values of ozone [*Sillman et al.*, 1990].

The plumes model may be used as an Eulerian or as a Lagrangian model. In the Lagrangian approach the model represents the evolution of a moving 400 x 480 $km^2$ air mass; emission rates and plume characteristics vary with location along the air mass trajectory. The two approaches give similar results for the evolution of ozone during an episode in the northeast United States [*Sillman et al.*, 1990]. In the study described below we adopt a Lagrangian approach. The model employs the two-layer structure described in section 3.1 above. Initial and boundary conditions are given in Table 1.

### 3.3. *Eulerian Grid Model.*

A fine-resolution (20 x 20 $km^2$) Eulerian grid model was used to explore the relationship between ozone and $NO_x$ in more detail and to make comparisons with observation. We adopted simple dynamical transports, as the focus here is on the chemical relationships. A single vertical layer with a height of 700 m was assumed, with a uniform wind of 3 m $s^{-1}$ blowing throughout the domain.

TABLE 1*a*. Initial and Boundary Conditions in Model Runs

| Species | Concentration* | Deposition Velocity, cm $s^{-1}$ |
|---|---|---|
| $O_3$ | 40 ppb | 0.6 |
| $NO_2$ | 0.23 ppb | 0.6 |
| NO | 0.023 ppb | 0.1 |
| CO | 200 ppb | NA |
| $CH_4$ | 1600 ppb | NA |
| $H_2$ | 500 ppb | NA |
| RH | 12.5 ppbC | NA |
| $H_2O_2$ | 1 ppb | 1.0 |
| PANs† | 0.08 ppb | 0.25 |
| $H_2O$ | 1.6 % | NA |
| $HNO_3$ | 0 | 2.5 |
| ROOH | 0 | 1.0 |
| Others | 0 | NA |

NA is not applicable.
* These values were used for initial, upwind and boundary conditions.
† PANs = peroxyacyl nitrates.

TABLE 1*b*. Partitioning of Hydrocarbons

| Species | Fraction* |
|---|---|
| $C_2H_6$ | 0.14 |
| $C_3H_8$ | 0.10 |
| ALK4 | 0.19 |
| ALK7 | 0.20 |
| $C_2H_4$ | 0.04 |
| $C_3H_6$ | 0.01 |
| BUTE | 0.01 |
| $C_6H_6$ | 0.05 |
| TOLU | 0.07 |
| XYLE | 0.03 |
| HCHO | 0.05 |
| ALD2 | 0.03 |
| RCHO | 0.05 |
| ACET | 0.02 |
| MEK | 0.01 |

Nomenclature follows *Lurmann et al.* [1986]. The partitioning of alkanes, alkenes and aromatics is based on rural ambient air measurements of *Arnts and Meeks* [1981]; the partitioning of other hydrocarbons is based on results of steady state calculations with the photochemical model.
* Values are given as a fraction of total carbon in RH.

TABLE 2. Partitioning of Hydrocarbon Emissions

| Species | Fraction* |
|---|---|
| $C_2H_6$ | 0.002 |
| $C_3H_8$ | 0.023 |
| ALK4 | 0.138 |
| ALK7 | 0.189 |
| $C_2H_4$ | 0.076 |
| $C_3H_6$ | 0.102 |
| BUTE | 0.136 |
| $C_6H_6$ | 0.020 |
| TOLU | 0.118 |
| XYLE | 0.196 |

* The partitioning of emissions is based on the ambient air measurements of *Arnts and Meeks* [1981].

Explicit diffusion was incorporated according to the prescription of *Gifford* [1982] with a diffusion coefficient of $10^4$ $m^2$ $s^{-1}$ to account for spreading of plumes from large scale sources. The model was run for 20 hours with a time step of 0.5 hour, and used the boundary and initial conditions given in Table 1. This model was designed to take full advantage of the spatial resolution available in the NAPAP emissions inventory [*EPA*, 1986*b*].

## 4. The Chemical Factors Affecting Ozone In Rural Air

We explored the sensitivity of ozone production to concentrations of $NO_x$ and hydrocarbons using the two-layer model described in the previous section. The model reproduces the observed diurnal behavior of ozone and $NO_x$ at rural sites, with highest concentrations of ozone and lowest concentrations of $NO_x$ in the afternoon [*Sillman*, 1987]. The calculations shown here represent the evolution of an air mass that receives uniform emissions of $NO_x$ and hydrocarbons. The model was run for 4 days, the duration of a typical ozone episode [*Logan*, 1989], with emissions of $NO_x$ and hydrocarbons selected to cover the range of concentrations of these species observed in ambient air.

Rural data for $NO_x$ are sparse, and many of the older measurements were made with instruments that suffered from interferences and that were not sufficiently sensitive to measure values below 2 ppb [*Fehsenfeld et al.*, 1988]. Analysis of the older data for summer suggests that median afternoon values of $NO_x$ at rural sites in the eastern United States are in the range <1 ppb to 4 ppb, with about 70% of values less than 8 ppb [*Logan*, 1989]. More recent high quality data for Scotia, Pennsylvania, indicate a median afternoon value of ~0.6 ppb [*Hubler et al.*, 1987]. Data for hydrocarbons are also exceedingly sparse. Typical rural values for the anthropogenic hydrocarbons appear to lie in the range 15 ppbC to 120 ppbC [*Sexton and Westberg*, 1984; *Seila et al.*, 1984; *Arnts and Meeks*, 1981; *Westberg et al.*, 1986; W. Lonneman, EPA, private communication, 1986]. Based on these data, we examine ozone chemistry for $NO_x$ concentrations in the range 0.2-8 ppb, and hydrocarbons (RH) in the range 5-120 ppbC. We show also the dependence of ozone on emission rate of isoprene, for fluxes in the range 0.1-4 x $10^{12}$ molecules C $cm^{-2}$ $s^{-1}$; this range was selected to encompass measured fluxes of isoprene [e.g., *Lamb et al.*, 1985, 1987].

Ozone concentrations are shown in Figure 2 for 1600 LT as a function of precursor emission rates and in Figure 3 as a function of the concentrations of $NO_x$ and anthropogenic hydrocarbons. Isoprene was omitted in these runs. Figures 2 and 3 show that there are two different photochemical regimes. When concentrations of $NO_x$ are low, <2 ppb, ozone increases as $NO_x$ increases but is almost insensitive to RH, as long as RH exceeds a certain threshold, which varies from ~10 ppbC for $NO_x$ = 0.25 ppb to ~50 ppbC for $NO_x$ = 2 ppb. For higher concentrations of $NO_x$, >4 ppb, ozone increases with increasing RH; if, in addition, the ratio of RH to $NO_x$ emissions is low (<2.5:1), ozone also decreases as $NO_x$ increases.

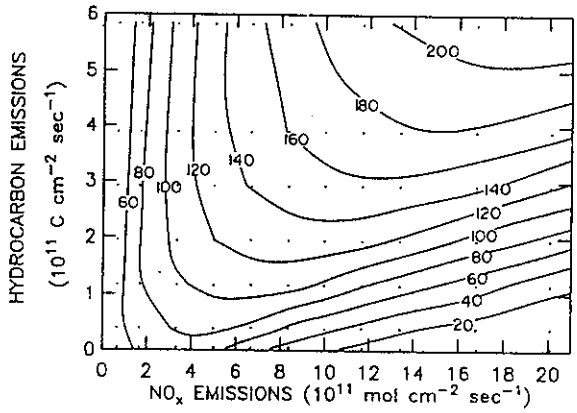


Fig. 2. Ozone in parts per billion as a function of the emission rates of $NO_x$ and anthropogenic hydrocarbons. Results of the two-layer model are shown for 1600 LT on the fourth day. Dots indicate the emission rates of $NO_x$ and hydrocarbon for individual simulations.

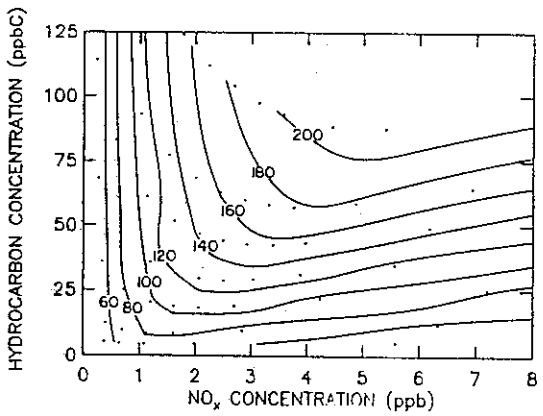


Fig. 3. Ozone in parts per billion as a function of the concentrations of $NO_x$ and hydrocarbons at 1600 LT, for the model runs shown in Figure 2. Dots indicate the concentrations of $NO_x$ and hydrocarbons at 1600 LT for individual simulations.

The behavior of ozone in these two $NO_x$ regimes may be understood by reference to equations (3)-(8), which give the dependence of OH and the production rate of ozone on concentrations of $NO_x$ and hydrocarbons. Although these relationships were derived from approximate solutions to the odd-hydrogen balance, we shall see that they are consistent with results of the complete photochemical model. Recall that the rate-limiting step for formation of ozone is the reaction of OH with RH (R5), and that $HO_2$ plays a key role in ozone formation by converting NO to $NO_2$. Figure 4 shows OH and $HO_2$ as functions of $NO_x$ and hydrocarbons, in the same format as Figure 3 for ozone. For low $NO_x$, OH increases as $NO_x$ increases, and decreases as RH increases, while $HO_2$ is much less sensitive to $NO_x$ and RH, as predicted by equations (6) and (7). Ozone also increases with $NO_x$ but is almost independent of RH, as predicted by equation (8) for the production of ozone. Equations (6)-(8) are valid when recombination of peroxy radicals provides the major sink for odd H, as discussed in section 2. Figure 5 shows the fraction of the odd-H sink attributed to net formation of peroxides as a function of $NO_x$ and hydrocarbons. Formation of peroxides provides more than 80% of the sink for odd-H when $NO_x$ <1 ppb, as shown in Figure 5. For the high $NO_x$ regime, $HO_2$ and OH decrease as $NO_x$ increases and increase as RH increases, as predicted by equations (2) and (3); production of ozone shows the same sensitivity to $NO_x$ and RH but is a stronger function of RH than is OH (see equation (4)). Equations (2)-(5) are valid when formation of $HNO_3$ provides the major sink for odd H. When $NO_x$ exceeds 4 ppb, and the RH:$NO_x$ emissions ratio is low (<2:1), formation of nitric acid provides over 50% of the sink for odd H, and peroxide formation provides less than 40% of the sink, as shown in Figure 5. Formation of PAN is a minor sink for odd H for the results shown here, <15%. The concentration of PAN as a function of $NO_x$ and hydrocarbons is shown in Figure 6.

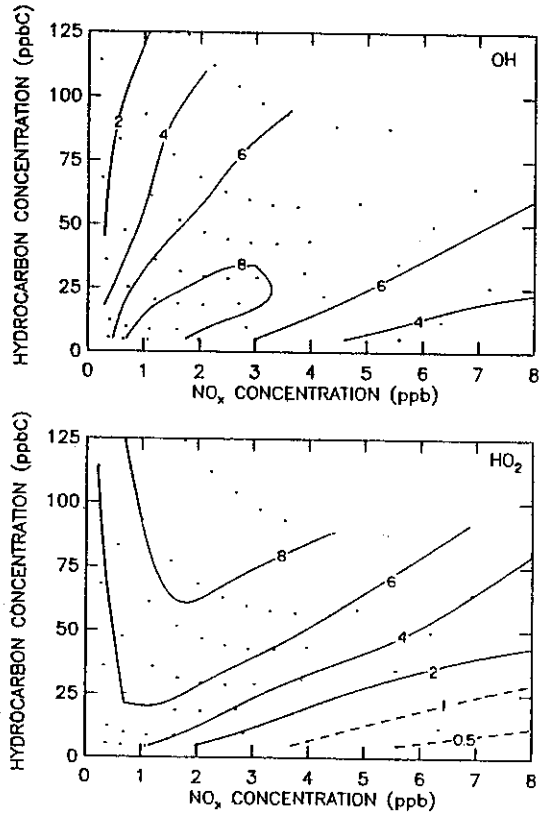


Fig. 4. (*a*) OH as a function of the concentrations of $NO_x$ and hydrocarbons at 1600 LT, for the model runs shown in Figures 2 and 3. Contours are given in units of $10^6$ molecules cm$^{-3}$. (*b*) $HO_2$ as a function of the concentrations of $NO_x$ and hydrocarbons at 1600 LT, for the model runs shown in Figures 2 and 3. Contours are given in units of $10^8$ molecules cm$^{-3}$.

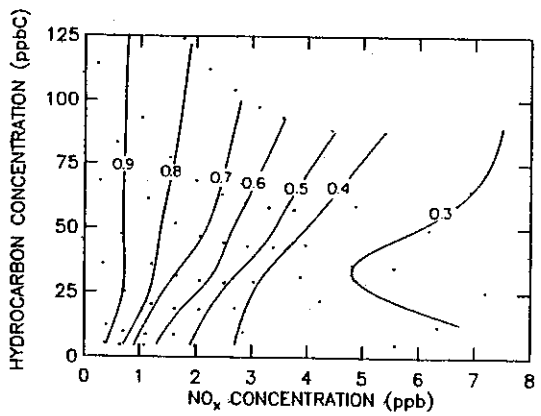


Fig. 5. The fraction of odd H that is removed by formation of peroxides as a function of the concentrations of $NO_x$ and hydrocarbons, for the model runs shown in Figures 2 and 3. This fraction is defined as ($R_{14}$ + $R_{15}$ - (the photolysis rate of H2O2 and ROOH))/$R_{14}$ + $R_{15}$ + $R_{10}$ + $R_{16}$), where $R_i$ refers to the rate of reaction Ri in the text.

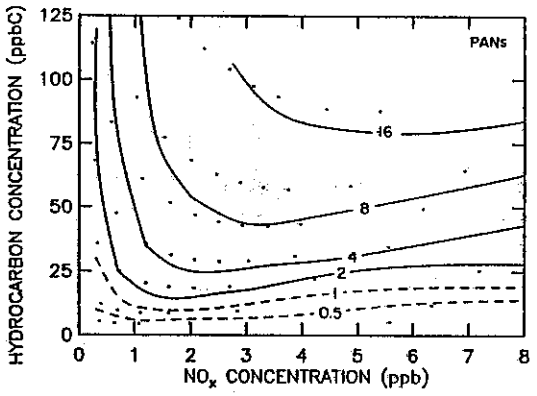


Fig. 6. Concentrations of PANs (PAN and its homologues) in parts per billion as a function of the concentrations of $NO_x$ and hydrocarbons at 1600 LT, for the model runs shown in Figures 2 and 3.

Concentrations of PAN increase as ozone increases (compare Figures 3 and 6), as expected from equation (10). It appears that the approximate equations derived in section 2 provide a reasonably accurate description of the chemistry of ozone for limiting cases of high and low $NO_x$.

Ozone concentrations are shown as a function of the emission rates of isoprene and $NO_x$ in Figure 7. Comparison of Figures 2 and 7 shows that the quantitative behavior of ozone as a function of emissions of $NO_x$ and RH (expressed in parts per billion carbon) is about the same, whether the hydrocarbons are provided by anthropogenic or biogenic emissions.

The results shown in Figure 3 suggest that afternoon concentrations of $NO_x$ must exceed ~1 ppb for ozone to exceed 100 ppb and that ozone is insensitive to the concentration of hydrocarbons for low values of $NO_x$. Median afternoon concentration of $NO_x$ were ~0.6 ppb at Scotia, Pennsylvania, the only rural site in the east for which high-quality data are available [*Hubler et al.*, 1987]. If this site is typical, the results in Figure 3 suggest that rural ozone levels are limited by the availability of $NO_x$. A similar conclusion was drawn by *Trainer et al.* [1987*a*], who modeled the Scotia data.

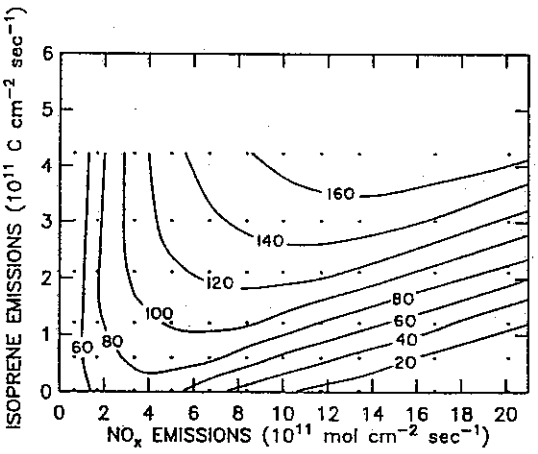


Fig. 7. Ozone in parts per billion as a function of the emission rates of $NO_x$ and isoprene. The model included 5 ppbC anthropogenic hydrocarbons. Results of the two-layer model are shown for 1600 LT on the fourth day. Dots indicate the emission rates of $NO_x$ and hydrocarbons for individual simulations.

## 5. Sensitivity of Rural Ozone to Emissions of $NO_x$ and Hydrocarbons

We have shown that the dependence of ozone on $NO_x$ is non linear for the concentration regime found in rural areas of the eastern United States. Emissions of $NO_x$ are spatially heterogeneous, with about 65% of emissions occurring in only 8% of the area [*Sillman et al.*, 1990]. We investigate therefore the sensitivity of rural ozone in the eastern United States with a model that allows for regions with high and low $NO_x$, the plumes model described by *Sillman et al.* [1990] and summarized in section 2. We have shown that this model is able to simulate rural atmospheric chemistry with an accuracy similar to that of a 40 x 40 $km^2$ Eulerian grid model but that it requires considerably less computer time [*Sillman et al.*, 1990]. In the other paper the plumes model was used to simulate an ozone episode in Ohio, Pennsylvania, and New York, and model results were compared to measurements of ozone at the surface and in the mixed layer, using a trajectory analysis available from *Clarke and Ching* [1983]. The plumes model simulated the buildup of ozone over the 4-day period quite well, reproducing both aircraft and surface data. The plumes model also simulates the buildup of ozone in an urban plume reasonably well [*Sillman et al.*, 1990].

We selected meteorological conditions for the present study typical of pollution episodes, with low wind speed (3 m $s^{-1}$), warm temperatures (an average value of 298 K), and an afternoon mixed layer height of 1500 m [*Evans et al.*, 1983; *Mukammal et al.*, 1985; *van Dop et al.*, 1987]. The rate of venting of the boundary layer into the free troposphere is not well known. During stagnation events the boundary layer is frequently capped by a subsidence inversion marked by sharp gradients in temperature, humidity, and pollutant concentrations [*Cho and Iribarne*, 1984; *Ching et al.*, 1988]; the rate of vertical transport through the inversion is slow. *Thompson and Lenchow* [1984] represent venting of the marine boundary layer with a vertical exchange coefficient of 0.3 cm $s^{-1}$ for daytime, based on the work of *Albrecht* [1979]. We adopted an exchange rate of 0.2 cm $s^{-1}$ in our simulations, corresponding to stagnant conditions, and we will explore the sensitivity of model results to the value assumed for this parameter.

We calculated the evolution of ozone in an air mass traversing the eastern United States from west to east. Two air mass trajectories were selected, as shown in Figure 8. These trajectories are typical of observed air motion during ozone episodes [e.g., *Clark and Ching*, 1983; *Evans et al.*, 1983]. Trajectory A begins in Illinois and traverses Indiana, Ohio and Pennsylvania, arriving in New York on the fourth day. Trajectory B starts in Missouri and traverses the Ohio River valley, reaching West Virginia by the fourth day.

The pattern of emissions is different for the two trajectories, although they both cross industrialized regions. Trajectory A crosses a heavily populated region of the United States and emissions are dominated by urban sources. There are fewer urban sources along trajectory B, but it traverses many more power plant sources. Total emissions of $NO_x$ are similar for the two trajectories, but emissions of anthropogenic hydrocarbons for trajectory A are more than twice the magnitude of those for trajectory B (see Table 2). Emissions from rural sources account for about 35% of $NO_x$ input along both trajectories. Finally, we note that the representative urban plumes for trajectory A correspond to larger cities than those for trajectory B.

Emission rates for $NO_x$ and anthropogenic hydrocarbons were taken from the NAPAP inventory, as discussed in section 3.

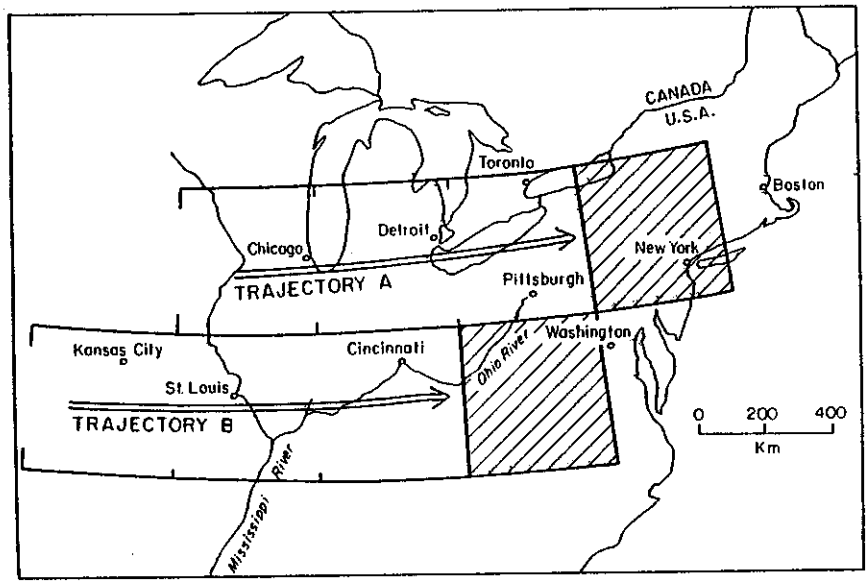


Fig. 8. Illustration of the two air mass trajectories used in the ozone episode simulations. The emissions for trajectory A are those for the box containing Chicago on the first day, and those for the boxes containing Detroit, Pittsburgh and New York on subsequent days. The shaded areas indicate the location of the simulated air masses on the fourth day of simulation.

Average emission rates for $NO_x$ are in the range 1.5 - 3.4 x $10^{11}$ molecules $cm^{-2}$ $s^{-1}$, for the 400 x 480 $km^2$ boxes traversed by the two trajectories, while emission rates for anthropogenic RH are in the range 3.5 - 15 x $10^{11}$ C atoms $cm^{-2}$ $s^{-1}$. These may be compared with our estimates for daytime average emissions of isoprene, 7.5 - 19 x $10^{11}$ C atoms $cm^{-2}s^{-1}$. Emission rates for individual boxes are given in Table 3.

We examined the sensitivity of ozone to precursor emissions by multiplying the emission rates for $NO_x$ and/or anthropogenic hydrocarbons given in the NAPAP inventory by a factor that ranged from 0.25 to 3 (case 1). Sensitivity to assumptions regarding emissions of isoprene were examined in case 2, temperature in case 3, and the venting rate of the boundary layer in case 4.

### 5.1. *Sensitivity of Ozone to $NO_x$ and Hydrocarbons, Case 1*

Ozone increased throughout the four days for each simulation, from an initial value of 40 ppb. Values are shown in Figure 9 for rural ozone on the fourth day and in Figure 10 for the peak value in the generic urban plume along the trajectory. This corresponds to values in the plume in the New York-Connecticut (NY-Conn) box (day 4 of the simulation) for trajectory A and that in the Ohio box (day 3 of the simulation) for trajectory B. The generic plume in the NY-Conn box has an initial width of 80 km (based on the New York metropolitan area) and initial $NO_x$ flux of 2.40 x $10^{12}$ molecules $cm^{-2}$ $s^{-1}$, while that in the Ohio box has an initial width of 40 km (based on Cincinnati) and a flux of 1.98 x $10^{12}$ molecules $cm^{-2}$ $s^{-1}$.

Rural ozone concentrations increase as $NO_x$ increases for the entire range of $NO_x$ emissions simulated here (see Figure 9). By contrast, emissions of anthropogenic hydrocarbons appear to have almost no effect on rural ozone for current emissions of $NO_x$, as estimated by NAPAP. Hydrocarbon emission rates become important only for $NO_x$ emissions a factor of 2 higher than NAPAP estimates. Simulations with NAPAP emissions give ozone concentrations of 86-92 ppb, typical of rural values found during ozone episodes [*Logan*, 1989]. Reducing $NO_x$ emissions by 50% reduces ozone levels by ~20 ppb while increasing $NO_x$ emissions by 50% produces a somewhat smaller increase in ozone.

The dependence of ozone on $NO_x$ in the urban plume is dramatically different from that for rural ozone (see Figure 10). Ozone increases with $NO_x$ only if $NO_x$ emissions are below the values

TABLE 3. Emissions of $NO_x$ and Hydrocarbons

| Grid Box | $NO_x$, $10^{11}$ molecules $cm^{-2}s^{-1}$ | RH, $10^{11}$ C atoms $cm^{-2}s^{-1}$ | Isoprene, $10^{11}$ C atoms $cm^{-2}s^{-1}$ |
|---|---|---|---|
| | | *Trajectory A*[*] | |
| 1 (IL) | 2.2 | 8.1 | 7.5 |
| 2 (MI) | 2.5 | 9.1 | 11.2 |
| 3 (PA) | 3.4 | 9.6 | 15.0 |
| 4 (NY) | 3.0 | 15.0 | 15.0 |
| | | *Trajectory B*[*] | |
| 5 (KC) | 1.5 | 3.5 | 7.5 |
| 6 (St.L) | 2.1 | 4.4 | 11.2 |
| 7 (CN) | 2.8 | 7.3 | 15.0 |
| 8 (WV) | 2.4 | 3.8 | 18.8 |

Emissions of $NO_x$ and anthropogenic hydrocarbons (RH) are average values for 24 hours in each grid box. Values for isoprene are average rates for 0600-1800 LT; nighttime emissions are zero.

[*] The boxes for each trajectory (see Figure 8) are numbered from west to east.

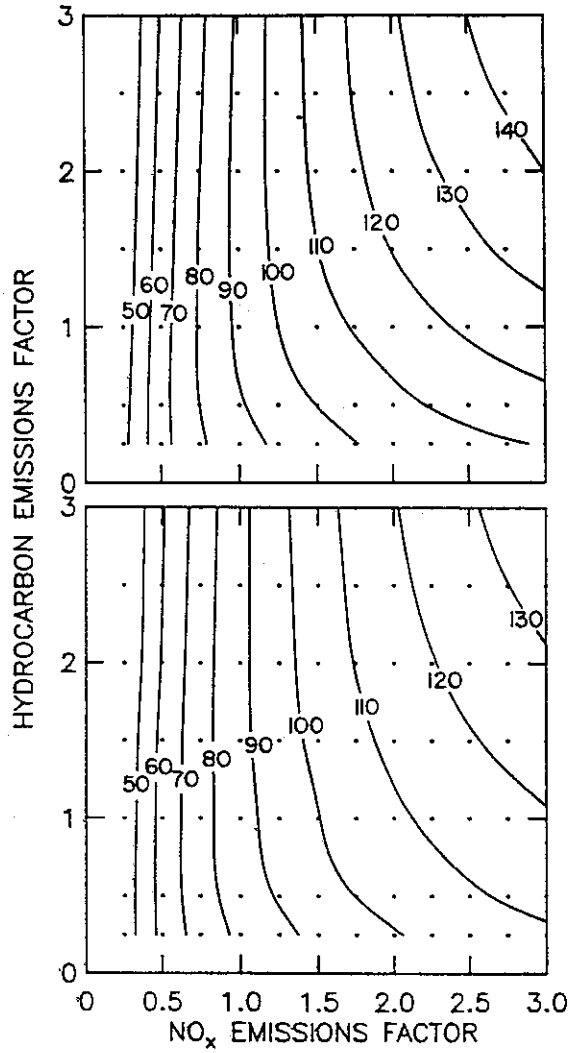


Fig. 9. Rural ozone in parts per billion as a function of $NO_x$ and hydrocarbon emissions. Results are shown for 1800 LT on the fourth day of ozone episode simulations with the plumes model for (top) trajectory A and (bottom) trajectory B. The numbers on the axes are the scaling factors by which the emissions in the NAPAP version 5.2 inventory were multiplied. The dots show the scaling factors for individual simulations on which the contours were based.

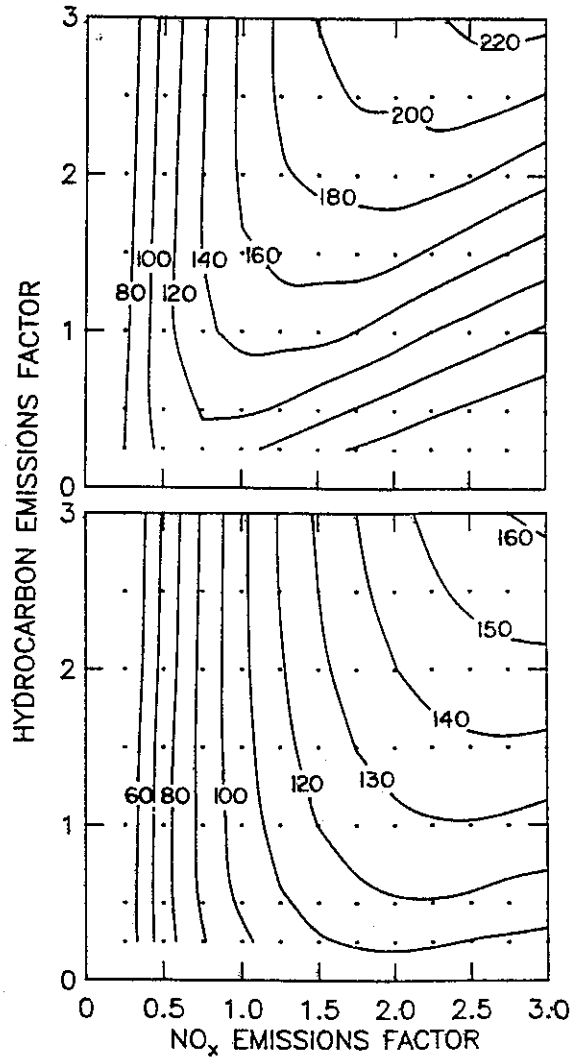


Fig. 10. Peak ozone in parts per billion in urban plumes for (top) the NY-Conn box on the fourth day and (bottom) the Ohio box on the third day, for the ozone episode simulations described in Figure 9.

given in the NAPAP inventory. For higher $NO_x$ emissions, ozone in urban plumes either remains constant, or decreases, as $NO_x$ emissions increase, and ozone increases strongly as hydrocarbon emissions increase. Simulations with NAPAP emissions give urban concentrations of 145 ppb in the NY-Conn region (trajectory A, fourth day) and 105 ppb in southern Ohio (trajectory B, third day). Reducing $NO_x$ emissions by 50% reduces ozone by 30-40 ppb. Increasing $NO_x$ emissions by 50% increases ozone by only 10 ppb in the Ohio urban plume; ozone in the NY-Conn plume would not increase at all unless hydrocarbon emissions are larger than those in the NAPAP inventory.

The regional model yields substantially different results for the urban plume than does a similar treatment for an isolated metropolitan area. Figure 11 shows the sensitivity of ozone in the NY-Conn plume to changes in emission rates for that single 400 x 480 $km^2$ box, as contrasted to results in Figure 10 for the effect of changes in emissions for the four 400 x 480 $km^2$ boxes along trajectory A. A 50% reduction in $NO_x$ emissions reduces ozone by

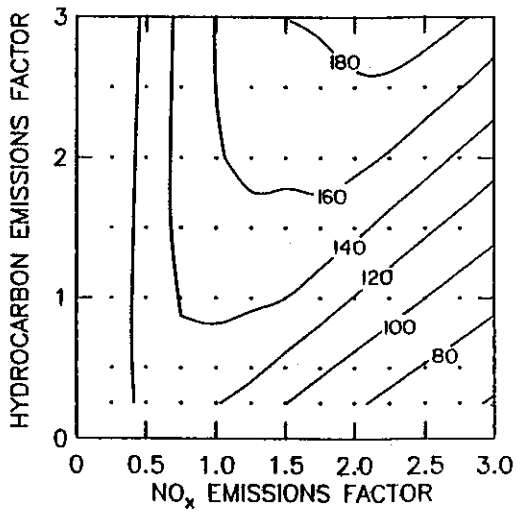


Fig. 11. Peak ozone in parts per billion in the urban plume in the NY-Conn box, for the fourth day of ozone episode simulations. Emissions in the NY-Conn box (see Figure 8) were multiplied by the scaling factors shown in the figure; emissions for the first three boxes of trajectory A were unscaled values from the NAPAP version 5.2 inventory.

about 15 ppb, as opposed to the reduction of 35 ppb predicted for uniform reduction of $NO_x$ for the entire trajectory. Predictions of the quantitative response of ozone in urban areas depends on details of the physical and chemical models adopted. The qualitative relationship shown in Figure 11, with a strong dependence on $NO_x$ and hydrocarbons, is similar to that predicted for urban areas by other models [e.g., *Finlayson-Pitts and Pitts*, 1986], but is different from that shown in Figure 9 for rural air. Increases in $NO_x$ emissions lead to increases in ozone in rural air, but increases in $NO_x$ emissions have little effect on ozone in urban plumes.

Ozone concentrations in rural air increase strongly with increasing $NO_x$ and are almost independent of RH because rural air corresponds to the low-$NO_x$ regime discussed in sections 2 and 4. Rural concentrations of $NO_x$ reach ~1 ppb for emissons of ~3 x $10^{11}$ molecules $cm^{-2}$ $s^{-1}$. In the urban plume, emissions and concentrations of $NO_x$ are higher by at least an order of magnitude, and the photochemistry is in a regime where formation of $HNO_3$ is becoming an important sink for $HO_x$. Urban ozone is less sensitive to local $NO_x$ emissions and more sensitive to RH, corresponding to the high-$NO_x$ regime discussed in sections 2 and 4. Export of ozone from urban and power plant plumes accounts for only 40% of the increase over background levels computed for the region. However, $NO_x$ from the plumes contributes significantly to photochemical production in rural areas, as this $NO_x$ interacts with reactive biogenic hydrocarbons.

We performed some detailed calculations that show that our results are not influenced by the simplifications inherent in the plumes model, which represents the distribution of $NO_x$ concentrations in a region using subgrid regions for rural air and for plumes from urban and power plant sources. Figure 12 (adapted from *Sillman et al.* [1990]) compares the cumulative distribution of $NO_x$ computed by the plumes model with $NO_x$ in an Eulerian grid model with resolution of 20 x 20 $km^2$. Afternoon concentrations of $NO_x$ are below 2 ppb for 80% of the region for the plumes model, and for 75% of the region for the 20 x 20 $km^2$ model; this is the regime where an increase in $NO_x$ causes an increase in ozone. If emissions and concentrations of $NO_x$ were increased by a factor of 2, at least 60% of the region would still be below 2 ppb for both models. The figure suggests that more detailed treatments (e.g., more than one generic plume of each type, overlapping plumes) may be needed in some cases, for example in a region with $NO_x$ emissions and concentrations substantially higher than those of the eastern United States.

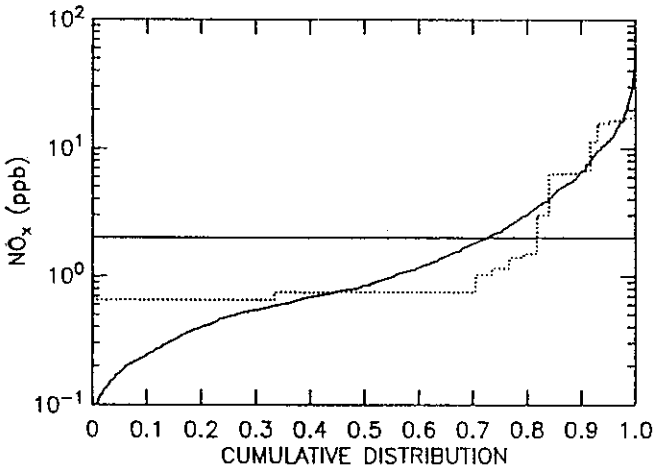


Fig. 12. Cumulative distribution for $NO_x$ calculated by the plumes model (dotted line) and by the 20 x 20 $km^2$ Eulerian grid model (solid line). Results are shown for 1400 LT for the two central boxes shown for trajectory A, Figure 8, and are taken from the work by *Sillman et al.* [1990].

### 5.2. *Sensitivity to Isoprene, Case 2*

Estimates for emission rates of isoprene are similar to NAPAP estimates for emissions of anthropogenic hydrocarbons for the regions included in this study. The daytime concentrations of isoprene in the simulations described above were about 1-2 ppbC. Isoprene is short lived, <2 hours, and exhibits significant vertical gradients in the boundary layer that are not represented in this model. Assuming that average values in the boundary layer are 0.25 times values at 5 m, based on the model studies of *Trainer et al.* [1987b], these correspond to surface values of 4-8 ppbC, within the range of observed values [*Arnts and Meeks*, 1981; *Altshuller*, 1983; *Trainer et al.* [1987a]. We ran a series of simulations with isoprene emissions reduced by a factor of 4, to examine the effect of isoprene on the results shown in Figure 9. Concentrations of isoprene were below 0.5 ppbC in these runs.

Concentrations of rural ozone in the simulations with low isoprene are lower than those for case 1 by a few parts per billion as shown in Figure 13. The effect of isoprene is greater for trajectory B where emissions of anthropogenic hydrocarbons are lower than for trajectory A. The rural ozone concentration for trajectory

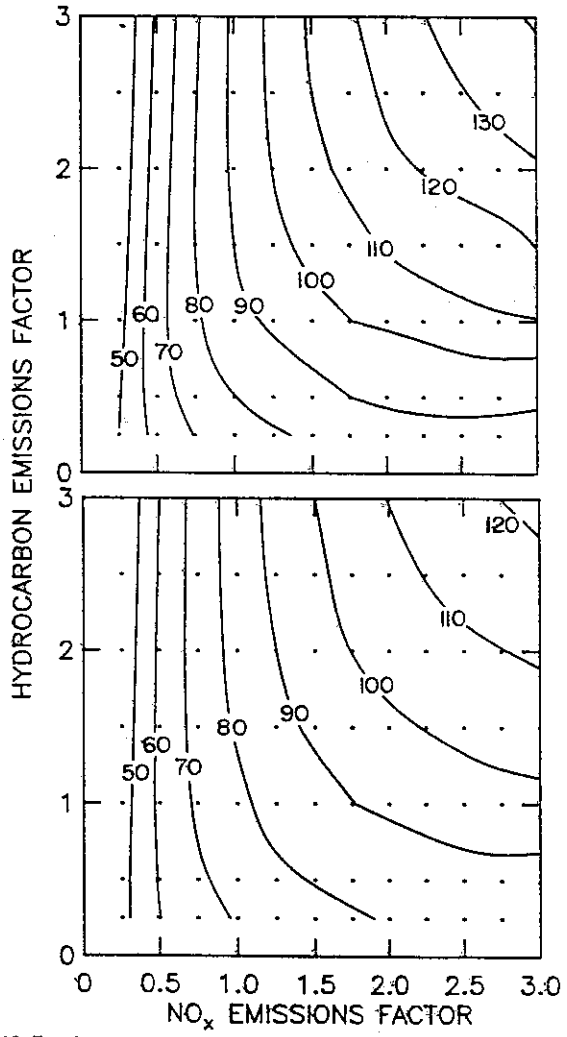


Fig. 13. Rural ozone in parts per billion as a function of emissions of $NO_x$ and anthropogenic hydrocarbons for case 2, isoprene emissions reduced by a factor of 4. The top panel is for trajectory A, the bottom panel for trajectory B. See Figure 9 for other details.

B drops from 86 to 78 ppb for NAPAP emissions, when isoprene emissions are reduced by a factor of 4. The dependence of ozone on $NO_x$ and hydrocarbons is the same for these simulations as for case 1, with only a slight shift with respect to the RH axis by the inclusion of lower concentrations of natural hydrocarbons in case 2. We showed earlier that anthropogenic and natural hydrocarbons have a similar effect on ozone, when expressed in units of carbon. Reducing isoprene emissions by a factor of 4 is equivalent to reducing total RH emissions by 28% for trajectory A and 43% for trajectory B. For case 2, ozone decreases slightly for decreases in RH, and ozone increases less than in case 1 as $NO_x$ is increased.

Concentrations for ozone in urban plumes in the simulations with low isoprene are also lower than those for case 1. This result is consistent with the findings of *Chameides et al.* [1988] who argued that ozone in Atlanta is influenced by emissions of isoprene. The qualitative behavior of ozone versus $NO_x$ and RH in the urban plumes is unaffected by the change in isoprene emissions.

### 5.3. *Sensitivity to Temperature, Case 3*

We conducted simulations with temperatures between 283 K and 303 K to examine the sensitivity of ozone to temperature. The concentration of water vapor was varied to maintain an afternoon relative humidity of 50%. All other parameters, including insolation, isoprene emissions and the diurnal variation of temperature were the same as in case 1. These simulations used NAPAP estimates for emissions of $NO_x$ and hydrocarbons.

Concentrations of ozone in rural air and in urban plumes are shown as a function of temperature in Figure 14 for trajectory A. Rural ozone increases by ~8 ppb for every 5 K increase in temperature, and plume ozone increases at a faster rate. Results show that concentrations of rural ozone above 80 ppb are unlikely for temperatures below ~290 K.

The effect of temperature on ozone is due primarily to the effect on the lifetime of PAN and its homologues. The lifetime of PAN towards thermal decomposition increases from 45 min at 298 K to ~ 9 hours at 283 K. Rural and plume concentrations of PAN increase with decreasing temperature, as shown in Figure 15 and Table 4. In the rural case, concentrations of $NO_x$ decrease at low temperatures, as the net formation rate of PANs increases; the decrease in $NO_x$, and the accompanying decrease in $HO_x$, cause a decrease in ozone as shown in Figures 3 and 4 (see also equations (6)-(8)). In the urban case, $NO_x$ levels may actually increase as temperatures decline, while $HO_x$ levels decline, since the net rate of removal of $NO_x$ into $HNO_3$ and PANs decreases (Table 5); here formation of PANs is important as a sink for $HO_x$ radicals. The lower levels of $HO_x$ reduce the rate for ozone formation at low-temperature in both cases. Lower water vapor in the low-temperature case also contributes to reduced $HO_x$ and slower ozone formation in urban plumes. However, in rural locations ozone increases when the water vapor content is reduced because the impact of water vapor as a sink for ozone and $NO_x$ outweighs its impact as a source for $HO_x$.

### 5.4. *Sensitivity to Vertical Transport, Case 4*

The simulations described above assumed an extremely low vertical exchange coefficient (0.2 cm $s^{-1}$). Cumulus convection can vent the boundary layer with an effective exchange rate as high as 1.0 cm $s^{-1}$ in some cases [*Cho and Iribarne*, 1984]. The effect of the venting rate on ozone is shown in Figure 16. Concentrations of rural ozone decline by 10 ppb as the venting rate increases from 0.2 cm $s^{-1}$ to 0.7 cm $s^{-1}$.

## 6. RELATIONSHIP BETWEEN OZONE AND NITROGEN OXIDES

We used a fine-resolution (20 x 20 $km^2$) Eulerian grid model to investigate in more detail the relationship between concentrations of ozone, $NO_x$, and $NO_y$ in rural air. $NO_y$ is the sum of all oxidized nitrogen species including $HNO_3$ and PANs. The model described in section 3.3 was applied to a region (800 x 480 $km^2$) of the northeastern United States, the two middle boxes of trajectory A (see Figure 8). The relationship between ozone and $NO_x$ for this region is shown in Figure 17; each point in the figure gives the value of ozone and $NO_x$ in one 20 x 20 $km^2$ grid box at 1800 LT. The high-resolution model shows an ozone increase as $NO_x$ increases, for $NO_x$ between 0.2 ppb and 2-3 ppb; ozone is independent of $NO_x$ for values from 2-3 ppb to 10 ppb and decreases as a function of $NO_x$ above 10 ppb. There is considerable scatter in the plot. This is to be expected, since the lifetime of $NO_x$, a few hours, is much shorter than that of ozone, a few days. Consequently, $NO_x$ in a particular area reflects local sources, while ozone is influenced by emissions, reactions and losses of $NO_x$ averaged over many time steps. The computed values for ozone and $NO_y$ are shown in Figure 18. Ozone increases as $NO_y$

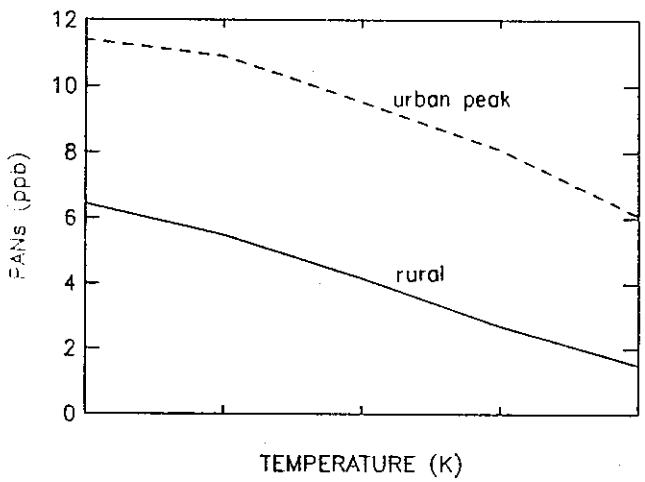


Fig. 14. Rural ozone (solid curve) and peak ozone concentrations (dashed curve) versus temperature for 4-day simulations for trajectory A, for NAPAP emissions.

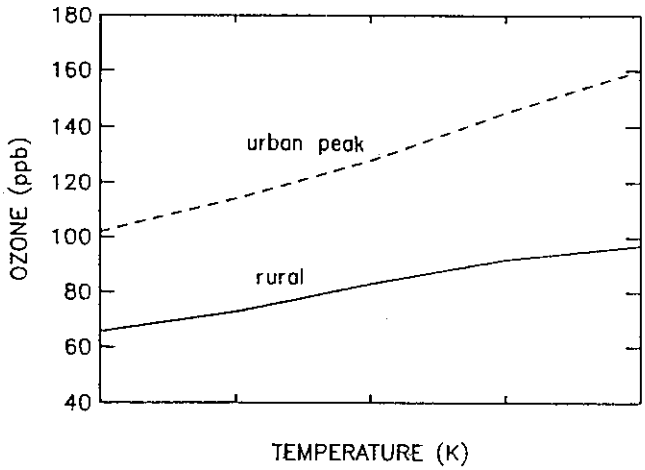


Fig. 15. Rural PAN (solid curve) and peak PAN (dashed curve) concentrations versus temperature for 4-day simulations for trajectory A, for NAPAP emissions. PAN includes peroxyacetylnitrate and its homologues in this figure.

TABLE 4. Effect of Temperature on $NO_y$ and $HO_x$

| | $NO_x$, ppb | PANs, ppb | $HNO_3$, ppb | OH, $10^6$ molecules $cm^{-3}$ | $HO_2$, $10^8$ molecules $cm^{-3}$ |
|---|---|---|---|---|---|
| | | | *Rural* | | |
| 298 K | 0.53 | 2.7 | 3.0 | 4.1 | 9.0 |
| 283 K | 0.24 | 6.2 | 1.7 | 1.5 | 6.4 |
| | | | *Urban* | | |
| 298 K | 10.8 | 6.3 | 9.4 | 6.3 | 3.1 |
| 283 K | 14.6 | 8.4 | 5.7 | 3.1 | 0.7 |

Concentrations are given for the fourth day of the plumes model simulation for trajectory A, at 1400 LT, for the rural and first urban plume boxes.

TABLE 5. Odd-Hydrogen Sinks

| | Peroxides | $HNO_3$ | PANs |
|---|---|---|---|
| | | *Rural* | |
| *298 K* | $1.39 \times 10^7$ | $4.95 \times 10^5$ | $6.33 \times 10^4$ |
| *283 K* | $7.17 \times 10^6$ | $6.44 \times 10^4$ | $6.44 \times 10^5$ |
| | | *Urban* | |
| 298 K | $1.82 \times 10^5$ | $1.57 \times 10^7$ | $8.89 \times 10^6$ |
| 283 K | $-8.72 \times 10^5$ * | $1.02 \times 10^7$ | $6.78 \times 10^6$ |

Net formation rates are given for all peroxides, nitric acid, and PAN and its homologues. Rates are for the fourth day of the plumes model simulations for trajectory A, for 1330-1400 LT, for the rural and first urban plume boxes. Units are molecules $cm^3 s^{-1}$.

* The net sink is negative if the odd hydrogen source from photolysis of peroxides exceeds the sink from formation of peroxides.

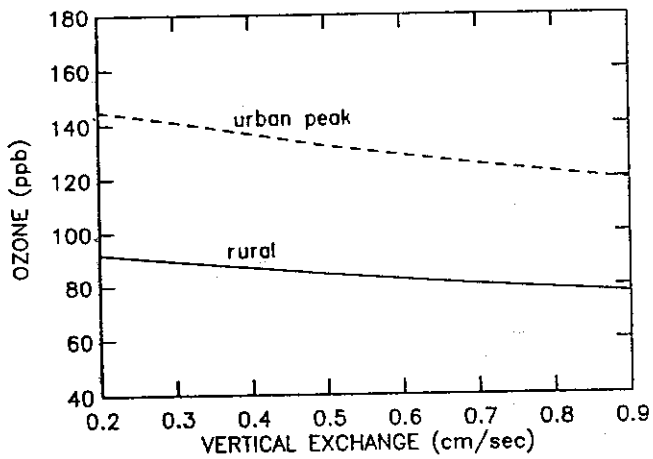


Fig. 16. Rural ozone (solid curve) and peak ozone (dashed curve) concentrations versus vertical exchange coefficient in centimeters per second for 4-day simulations for trajectory A for NAPAP emissions.

increases for values of $NO_y$ between 0.2 and ~15 ppb and decreases as $NO_y$ increases for values above 20 ppb. There is considerably less scatter in this plot than in the $NO_x$ plot. The lifetime of $NO_y$ is about a day (in the absence of rainfall), similar to that of ozone; both are removed by deposition. The $NO_y$ concentration reflects integrated emissions of nitrogen oxides received by the air mass, and the model results in Figure 18 suggest that ozone and $NO_y$ should be highly correlated, at least for values of $NO_y$ below 10 ppb.

Concurrent measurements of ozone, $NO_x$, and $NO_y$ have been made at two sites in the United States, Niwot Ridge, Colorado, and Scotia, Pennsylvania. The data for ozone and $NO_x$ from Niwot Ridge are shown in Figure 17 [*Parrish et al.*, 1986; *Liu et al.*, 1987]. The solid line is based on all the afternoon data, while the circles represent data for clear sky conditions. At this remote site, which is influenced by aged urban air, ozone increases as $NO_x$ increases, for $NO_x$ values up to about 5 ppb. Results for Scotia are similar, except that ozone increases as $NO_x$ increases only up to about 2 ppb (F. C. Fehsenfeld et al., private communication, 1987). Data for ozone and $NO_y$ from Niwot Ridge are shown in Figure 18; the solid line is based on daytime values [*Fahey et al.*, 1986]. Ozone increases as $NO_y$ increases, for values up to 8 ppb. The variability in the plot of data for ozone versus $NO_y$ is much less than that for ozone versus $NO_x$. Model results appear to be consistent with the observed relationship between ozone and nitrogen oxides.

## 7. CONCLUSIONS

Model studies presented in sections 4 and 5 suggest that ozone in rural air depends strongly on concentrations of $NO_x$ but is almost independent of the amount of hydrocarbons present. This behavior is different from that for urban air, where ozone depends on both $NO_x$ and hydrocarbons. We showed that this behavior is consistent with our understanding of the chemical mechanisms of ozone formation and is consistent also with observations in a rural setting. Ozone concentrations in urban plumes appear to be sensitive to upwind regional-scale emissions in addition to urban emissions. It has been suggested that NAPAP estimates for emissions of RH may be too small by a factor of 2 [*Ching et al.*, 1987]. Inspection of Figures 9, 10 and 12 shows that our conclusions would be unaffected by such an error.

Isoprene appears to provide an important source of hydrocarbons in the eastern United States in summer [*Lamb et al.*, 1987; *Trainer et al.*, 1987a]. Our conclusions regarding the impact of $NO_x$ and hydrocarbons in rural air are not, however, strongly dependent on our assumptions regarding the flux of isoprene. Concentrations of other hydrocarbons (primarily derived from anthropogenic sources) are greater than 15 ppbC and are often larger than 50 ppbC [*Arnts and Meeks*, 1981; *Altshuller*, 1983; *Sexton and Westberg*, 1984; *Seila et al.*, 1984; *Westberg et al.*, 1986].

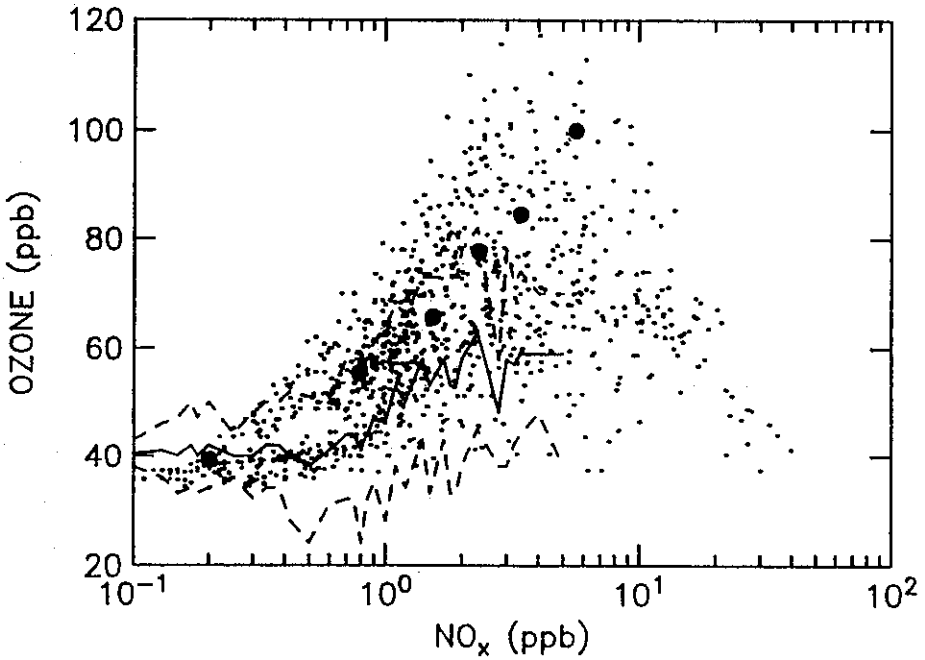


Fig. 17. Ozone versus $NO_x$ concentrations at 1800 LT for each 20 x 20 $km^2$ grid for the one-layer model. The model domain is the center two boxes of trajectory A, Figure 8. The lines indicate the average and standard deviation of observed ozone concentrations as a function of observed $NO_x$ at Niwot Ridge, Colorado based on data for summer afternoons, 1500-2000 LT, June 1 to August 31 [*Parrish et al.*, 1986]. The solid circles are based on the same data set and show data selected for clear sky conditions, from 1400 to 1900 LT [*Liu et al.*, 1987].

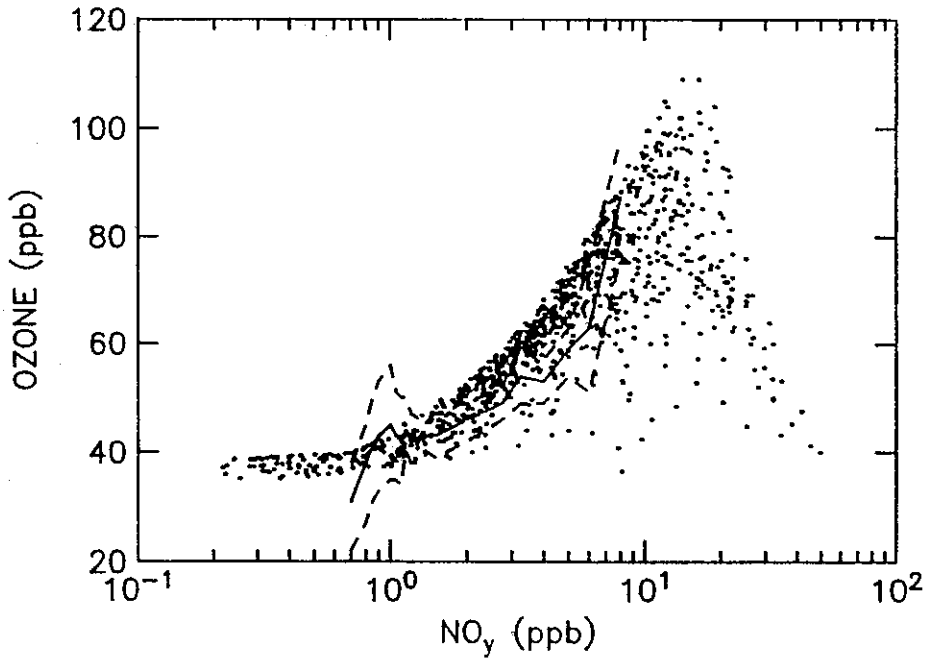


Fig. 18. Ozone versus $NO_y$ concentrations at 1800 LT for each 20 x 20 $km^2$ grid for the one-layer model. $NO_y$ is defined as the sum of all oxidized nitrogen species. The model domain is the center two boxes of trajectory A, Figure 8. The lines indicate the average and standard deviation of observed ozone concentrations as a function of observed $NO_y$ at Niwot Ridge, Colorado, based on daytime summer data, 0800-1800 LT, June 28 to July 20, 1984 [*Fahey et al.*, 1986].

Reliable data for $NO_x$ at rural locations in the east are few, as discussed above, but there are indications that afternoon values are frequently below 2 ppb, consistent with our simulations. If this is indeed the case for most rural locations in the eastern United States, then rural ozone is limited by the availability of $NO_x$. Concentrations of $NO_x$ as low as 1 ppb permit significant photochemical production of ozone in concert with either anthropogenic or biogenic hydrocarbons, as shown in Figures 3 and 16, and in the studies of *Trainer et al.* [1987*a*]. Sensitivities to $NO_x$ are markedly different in rural air, as compared to urban air. These results

may have important implications for attempts to regulate emissions, in order to reduce photochemical oxidant levels in urban and rural areas.

*Acknowledgments.* This work was supported by the Coordinating Research Council, Incorporated (Project AP-9), the National Science Foundation (ATM84-13153), and the Environmental Protection Agency (R814535-01-0).

## REFERENCES

Albrecht, B. A., A model of the thermodynamic structure of the trade wind boundary layer, II, Applications, *J. Atmos. Sci., 36*, 90-98, 1979.

Altshuller, A. P., Review: Natural volatile organic substances and their effect on air quality in the United States, *Atmos. Environ., 17*, 2131-2165, 1983.

Arnts, R. A., and S. A. Meeks, Biogenic hydrocarbon contribution to ambient air in selected areas, *Atmos. Environ., 15*, 1643-1651, 1981.

Atkinson, R., Kinetics and mechanisms of the gas-phase reactions of the hydroxyl radical with organic compounds under atmospheric conditions, *Chem. Rev., 86*, 69-201, 1986.

Attmannspacher, W., R. Hartmannsgruber, and P. Lang, Langzeittendenzen des Ozons der Atmosphare aufgrund der 1967 begonnenen Ozonmessreihen am Meteorologischen Observatorium Hohenpeissenberg, *Meteorol. Rdsch., 37*, 193-199, 1984.

Chameides, W. L., R. W. Lindsay, J. Richardson, and C. S. Kiang, The role of biogenic hydrocarbons in urban photochemical smog: Atlanta as a case study, *Science, 241*,1473-1475, 1988.

Ching, J. C. S., J. A. Novak, K. L. Schere, and N. V. Gilliani, Reconciling urban VOC/$NO_x$ emission inventories with ambient concentration data, paper presented at the 80th Meeting of the Air Pollution Control Association, New York, 1987.

Ching, J. K. S., S. T. Shipley, and E. V. Browell, Evidence for cloud venting of mixed layer ozone and aerosols, *Atmos. Environ., 22*, 225-242, 1988.

Cho, H., and J. V. Iribarne, Effect of cumulus cloud systems on the vertical distribution of air pollutants, in *The Meteorology of Acid Deposition*, edited by P. J. Samson, pp. 127-139, Air Pollution Control Association, Pittsburgh, Penn., 1984.

Clarke, J. F., and J. K. S. Ching, Aircraft observations of regional transport of ozone in the northeastern United States, *Atmos. Environ., 17*, 1703-1712, 1983.

Cox, R. A., and M. J. Roffey, Thermal decomposition of peroxyacetylnitrate in the presence of nitric oxide, *Environ. Sci. Technol., 11*, 900-906, 1977.

Cox, R. A., A. E. J. Eggleton, R. G. Derwent, J. E. Lovelock, and D. H. Pack, Long range transport of photochemical ozone in northwestern Europe, *Nature, 225*, 118-121, 1975.

Decker, C. E., L. A. Ripperton, J. J. B. Worth, F. M. Vukovich, W. D. Bach, J. B. Tommerdahl, F. Smith, and D. E. Wagoner, Formation and transport of oxidants along Gulf coast and in northern U. S., *EPA-450/3-76-003*, U.S. Environ. Prot. Agency, Research Triangle Park, N. C., 1976.

DeMore, W. B., J. J. Margitan, M. J. Molina, R. T. Watson, D. M. Golden, R. F. Hampson, M. J. Kurylo, C. J. Howard, and A. R. Ravishankara, Chemical kinetics and photochemical data for use in stratospheric modeling, *Jet Propul. Lab. Publ. 85-37*, Calif. Inst. of Technol., Pasadena, Calif., 1985.

Environmental Protection Agency, (EPA), Air quality criteria for ozone and other photochemical oxidants, *EPA/600/8-84-020-CF and EPA/600/8-84-020-EF*, U.S. Environ. Prot. Agency, Research Triangle Park, N. C., 1986*a*.

Environmental Protection Agency, (EPA), Development of the 1980 NAPAP emissions inventory, *EPA/600/7-86-057a*, U.S. Environ. Prot. Agency, Research Triangle Park, N. C., 1986*b*.

Evans, G. F., P. Finkelstein, B. Martin, N. Possiel, and M. Graves, Ozone measurements from a network of remote sites, *J. Air Pollut. Control. Assoc., 33*, 291-296, 1983.

Fahey, D. W., G. Hubler, D. D. Parrish, E. J. Williams, R. B. Norton, B. A. Ridley, H. B. Singh, S. C. Liu, and F. C. Fehsenfeld, Reactive nitrogen species in the troposhere: Measurements of NO, $NO_2$, $HNO_3$, particulate nitrate, peroxyacetylnitrate (PAN), $O_3$ and total reactive odd nitrogen ($NO_y$) at Niwot Ridge, Colorado, *J. Geophys. Res., 91*, 9781-9793, 1986.

Fehsenfeld, F. C., D. D. Parrish, and D. W. Fahey, The measurement of $NO_x$ in the non-urban troposphere, in *Proceedings of the NATO Advanced Research Workshop on Regional and Global Ozone and its Environmental Consequences, NATO ASI Ser. C, vol. 227*, edited by I. S. A. Isaksen, pp. 185-216, Reidel, Hingham, Mass., 1988.

Feister, U., and W. Warmbt, Long-term measurements of surface ozone in the German Democratic Republic, *J. Atmos. Chem., 5*, 1-21, 1987.

Finlayson-Pitts, B. J., and J. N. Pitts, Jr., *Atmospheric Chemistry: Fundamentals and Experimental Techniques*, Wiley-Interscience, New York, 1986.

Flowers, E. C., R. A. McCormick, and K. R. Kurfis, Atmospheric turbidity over the United States, 1961-1966, *J. Appl. Meteorol., 8*, 955-962, 1969.

Folinsbee, L. J., W. F. McDonnell, and D. H. Horstman, Pulmonary function and symptom responses after 6.6-hour exposure to 0.12 ppm ozone with moderate exercise, *J. Air. Pollut. Control. Assoc., 38*, 28-35, 1988.

Gifford, F. A., Horizontal diffusion in the atmosphere: A Lagrangian-dynamical theory, *Atmos. Environ., 16*, 505-512, 1982.

Guicherit, R., and H. van Dop, Photochemical production of ozone in Western Europe (1971-1978) and its relation to meteorology, *Atmos. Environ., 11*, 145-155, 1977.

Heck, W. W., O. C. Taylor, R. Adams, G. Bingham, J. Miller, E. Preston, and L. Weinstein, Assessment of crop loss from ozone, *J. Air Pollut. Control. Assoc., 32*, 353-361, 1982.

Hendry, D. G., and R. A. Kenley, Atmospheric chemistry of peroxynitrates, in *Nitrogenous Air Pollutants: Chemical and Biological Implications*, Chap. 7, edited by D. Grosjean, Ann Arbor Science, Ann Arbor, Mich., 1979.

Hov, O., E. Hesstvedt, and I. S. A. Isaksen, Long-range transport of tropospheric ozone, *Nature, 273*, 341-344, 1978.

Hubler, G., D. W. Fahey, D. D. Parrish, E. J. Williams, M. P. Buhr, R. B. Norton, C. M. Curran, P. C. Murphy, F. C. Fehsenfeld, B. A. Ridley, J. D. Shetter, and B. W. Gandrud, Partitioning of reactive odd species in the tropospheric boundary layer, paper presented at the 6th International Symposium of the Commission on Atmospheric Chemistry and Global Pollution of the International Association of Meteorology and Atmospheric Physics, Peterborough, Canada, August 23-29, 1987.

Isaksen, I. S. A., O. Hov, and E. Hesstvedt, Ozone generation over rural areas, *Environ. Sci. Technol., 12*, 1279-1284, 1978.

Jacob, D. J., and S. C. Wofsy, Photochemistry of biogenic emissions over the Amazon forest, *J. Geophys. Res., 93*, 1477-1486, 1988.

Kleinman, L. I., Photochemical formation of peroxides in the boundary layer, *J. Geophys. Res., 91*, 10889-10904, 1986.

Lamb, B., H. Westberg, G. Allwine, and T. Quarles, Biogenic hydrocarbon emissions from deciduous and coniferous trees in the United States, *J. Geophys. Res., 90*, 2380-2390, 1985.

Lamb, B., A. Guenther, D. Gay, and H. Westberg, A national inventory of biogenic hydrocarbon emissions, *Atmos. Environ., 21*, 1695-1705, 1987.

Lefohn, A. S., and V. C. Runeckles, Establishing standards to protect vegetation - Ozone exposure/dose considerations, *Atmos. Environ., 21*, 561-568, 1987.

Lin, X., M. Trainer, and S. C. Liu, On the nonlinearity of tropospheric ozone production, *J. Geophys. Res., 93*, 15879-15888, 1988.

Liu, S. C., M. Trainer, F. C. Fehsenfeld, D. D. Parrish, E. J. Williams, D. W. Fahey, G. Hubler, and P. C. Murphy, Ozone production in the rural troposphere and implications for regional and global ozone distributions, *J. Geophys. Res., 92*, 4191-4207, 1987.

Logan, J. A., Tropospheric ozone: Seasonal behavior, trends and anthropogenic influence, *J. Geophys. Res., 90*, 10463-10482, 1985.

Logan, J. A., Ozone in rural areas of the United States, *J. Geophys. Res.*, *94*, 8511-8532, 1989.

Logan, J. A., M. J. Prather, S. C. Wofsy and M. B. McElroy, Tropospheric chemistry: A global perspective, *J. Geophys. Res.*, *86*, 7210-7254, 1981.

Lurmann, F. W., A. C. Lloyd, and R. Atkinson, A chemical mechanism for use in long-range transport/acid deposition computer modeling, *J. Geophys. Res.*, *91*, 10905-10936, 1986.

Matthews, E., Global vegetation and land use: New high-resolution data bases for climate studies, *J. Clim. Appl. Meteorol.*, *22*, 474-487, 1983.

Mukammal, E. I., H. H. Neumann, and T. R. Nichols, Some features of the ozone climatology of Ontario, Canada and possible contributions of stratospheric ozone to surface concentrations, *Arch. Meteorol. Geophys. Bioklimatol., Ser. A*, *34*, 179-211, 1985.

Parrish, D. D., D. W. Fahey, E. J. Williams, S. C. Liu, M. Trainer, P. C. Murphy, D. L. Albritton, and F. C. Fehsenfeld, Background ozone and anthropogenic ozone enhancement at Niwot Ridge, Colorado, *J. Atmos. Chem.*, *4*, 63-80, 1986.

Research Triangle Institute, Investigation of rural oxidant levels as related to urban hydrocarbon control strategies, *EPA-450/3-75-036*, Environ. Prot. Agency, Research Triangle Park, N. C., 1975.

Seila, R. L., R. R. Arnts, and J. W. Buchanan, Atmospheric volatile hydrocarbon composition at five remote sites in northwestern North Carolina, in *The Environmental Impact of Natural Hydrocarbon Emissions*, edited by V. Aneja, pp. 125-133, Air Pollution Control Association, Pittsburgh, Penn., 1984.

Selby, K., A modeling study of atmospheric transport and photochemistry in the mixed layer during anticyclonic episodes in Europe, II, Calculations of photo-oxidant levels along air trajectories, *J. Clim. Appl. Meteorol.*, *26*, 1317-1338, 1987.

Sexton, K., and H. Westberg, Non-methane hydrocarbon composition of urban and rural atmospheres, *Atmos. Environ.*, *18*, 1125-1132, 1984.

Sillman, M. S., Models for regional scale photochemical production of ozone, Ph.D. thesis, Harvard Univ., Cambridge, Mass., 1987.

Sillman, S., J. A. Logan, and S. C. Wofsy, A regional-scale model for photochemical production of ozone in the United States with sub-grid representation of urban and power plant plumes, *J. Geophys. Res.*, in press, 1990.

Singh, H. B., J. R. Martinez, D. G. Hendry, R. J. Jaffe, and W. B. Johnson, Assessment of the oxidant-forming potential of light saturated hydorcarbons in the atmosphere, *Environ. Sci. Technol.*, *15*, 113-119, 1981.

Skarby, L., and G. Sellden, The effects of ozone on crops and forests, *Ambio*, *13*, 68-72, 1984.

Thompson, A. M., and D. H. Lenchow, Mean profiles of trace reactive species in the unpolluted marine surface layer, *J. Geophys. Res.*, *89*, 4788-4796, 1984.

Trainer, M., E. J. Williams, D. D. Parrish, M. P. Buhr, E. J. Allwine, H. H. Westberg, F. G. Fehsenfeld, and S. C. Liu, Models and observations of the impact of natural hydrocarbons on rural ozone, *Nature*, *329*, 705-707, 1987*a*.

Trainer, M., E. Y. Hsie, S. A. McKeen, R. Tallamraju, D. D. Parrish, F. C. Fehsenfeld, and S. C. Liu, Impact of natural hydrocarbons on hydroxyl and peroxy radicals at a remote site, *J. Geophys. Res.*, *92*, 11,879-11,894, 1987*b*.

van Dop, H., J. F. den Tonkelaar, and F. E. J. Briffa, A modeling study of atmospheric transport and photochemistry in the mixed layer during anticyclonic episodes in Europe, I, Meteorology and air trajectories, *J. Clim. Appl. Meteorol.*, *26*, 1305-1316, 1987.

van Ulden, A. P., and A. A. M. Holtslag, Estimation of atmospheric boundary-layer parameters for diffusion applications, *J. Clim. Appl. Meteorol.*, *24*, 1196-1207, 1985.

Volz, A., and D. Kley, Evaluation of the Montsouris series of ozone measurements made in the nineteenth century, *Nature*, *332*, 240-242, 1988.

Vukovich, F. M., W. D. Bach, B. W. Crissman, and W. J. King, On the relationship between high ozone in the rural surface layer and high pressure systems, *Atmos. Environ.*, *11*, 967-983, 1977.

Warmbt, W., Results of long term measurements of near surface ozone in the GDR, *Z. Meteorol.*, *29*, 24-31, 1979.

Wesely, M. L., Turbulent transfer of ozone to surfaces common in the eastern United States, in *Trace Atmospheric Constituents: Properties, Transformations and Fates*, edited by S. E. Schwartz, pp. 345-370, John Wiley, New York, 1983.

Westberg, H. H., J. C. Farmer, B. K. Lamb, D. W. Arlander, and E. J. Allwine, Relationship between ambient concentrations of hydrocarbons, aldehydes, and organic acids (abstract), *Eos Trans. AGU*, *67*, 891, 1986.

Wolff, G. T., and P. J. Lioy, Development of an ozone river associated with synoptic scale episodes in the eastern United States, *Environ. Sci. Technol.*, *14*, 1257-1261, 1980.

Wolff, G. T., P. J. Lioy, G. D. Wight, R. E. Meyers, and R. T. Cederwall, An investigation of long range transport of ozone across the mid western and eastern United States, *Atmos. Environ.*, *11*, 797-802, 1977.

Woodman, J. N., and E. B. Cowling, Airborne chemicals and forest health, *Environ. Sci. Technol.*, *21*, 120-126, 1987.

J. A. Logan and S. C. Wofsy, Department of Earth and Planetary Sciences and Division of Applied Sciences, Harvard University, Pierce Hall 29 Oxford Street, Cambridge, MA 02138.

S. Sillman, Department of Atmospheric, Oceanic, and Space Sciences, University of Michigan, Ann Arbor, MI 48109-2143.

(Received January 10, 1989;
revised July 17, 1989;
accepted July 17, 1989.)